

Investigation of the Surface Roughness of Micromilled 316L Stainless Steel Fabricated by FDM/FFF Technology

Suleiman Obeidat, Jacob Nicholas, Jhoana Alfaro, Syed Faruqui, Iftekhar Basith

Department of Engineering Technology, Sam Houston State University

Abstract

This study explores how 3D printing parameters, specifically raster angle and layer thickness, affect the surface finish of 316L stainless steel parts after micromilling. The parts were printed using BASF Ultrafuse 316L filament on a MakerBot Method X printer, with raster angles of 0°, 30°, and 45°, and layer thicknesses of 0.1 mm and 0.2 mm. Prints were made in flat and edge orientations, then sintered in a furnace to create solid metal parts. After sintering, micromilling was performed in three directions (0°, 90°, and 180°) to investigate the surface finish of the 3D printed parts. Surface roughness was then measured to understand the impact of the different printing parameters. The results showed that layer thickness had the most noticeable effect on roughness, especially at 90°. Raster angle and build orientation also seemed to play a role, but their influence wasn't always consistent or statistically significant across all samples.

Keywords: Additive manufacturing; FDM/FFF; 316L Stainless steel; Machining, Surface roughness.

Introduction

The increasing interest in metal additive manufacturing, particularly using fused deposition modeling (FDM), has opened new possibilities for producing cost-effective metal parts like 316L stainless steel. One of the main challenges with this approach lies in achieving a good surface finish. Surface finish is important for different industries such as automotive, oil and gas, and aerospace. This review explores recent studies focusing on how 3D printing parameters, especially raster angle, layer thickness, and part orientation, affect surface roughness after micro-milling. Cerlincă et al. (2024) investigated how ironing parameters during FDM printing influence the surface quality of green and sintered 316L parts. They found that closer ironing spacing and higher speeds can significantly improve the top surface finish before and after sintering. These results suggest that pre-processing strategies like ironing can reduce the burden on post-machining. O'Connor et al. (2024) used an Analysis of Variance (ANOVA) approach to optimize FDM settings for 316L/PLA composite filaments. Their findings revealed that printing with 0.1 mm and slower speeds yielded the smoothest green parts. Martignoni et al. (2024) examined printing parameters for metal FFF using 316L stainless steel. They achieved green part densities above 99%. The process proved its effectiveness for producing complex lattice geometries with proper design constraints. Spiller et al. (2023) investigated the fabrication of 316L stainless steel components using Material Extrusion Additive Manufacturing with BASF Ultrafuse filament. The study achieved up to 95% relative density in sintered parts and reported tensile strengths between 450–500 MPa with ductility around 10–15%, comparable to metal injection molding. Boschetto et al. (2022) examined the surface roughness of 316L stainless steel parts fabricated using Metal Fused Filament Fabrication (FFF). They found that deposition angle significantly influenced surface roughness, with sintering further altering surface profiles. Kedziora et al. (2022) evaluated 316L and 17-4 PH stainless steel parts made via metal FFF and SLM. They found that FFF parts had lower strength and higher porosity but offered acceptable performance for non-critical applications. Caminero et al. (2021) assessed 316L stainless steel parts produced via FFF using BASF Ultrafuse material. They focused on building orientation and printing strategy. They achieved components with <2 % porosity and found that flat and on-edge orientations significantly improved mechanical performance (up to 22 % higher tensile strength and 118 % greater elongation) compared to upright builds. Galati and Minetola (2019) analyzed 17-4 PH stainless steel parts fabricated using the Atomic Diffusion Additive Manufacturing (ADAM) process. They found that part geometry and layer thickness significantly influenced porosity and surface quality. Obeidat et al. (2024) studied the impact of the raster angle on the apparent density and the mechanical properties of 316L stainless steel 3D printed parts using FDM technology. Liu et al. (2020) introduced a fused deposition modeling and sintering (FDMS) approach to fabricate metal parts using 316L/POM composite filaments. They found that while the method yields dense parts with acceptable geometry, porosity, and shrinkage limit mechanical strength. Ren et al. (2017) optimized process parameters for extrusion-based metal 3D printing using a copper–PW/LDPE/SA binder system. They found that infill degree and sintering temperature significantly affect green strength and final part hardness. The surface roughness of 3D printed parts has been extensively studied, but there is a lack of research on the interaction between 3D printing parameters and the surface roughness of 3D printed parts after machining. This is the motivation of this study, where the interaction between the raster angle, layer thickness,

printing orientation, and surface roughness is investigated. By linking FDM/FFF printing parameters with post-machined surface quality, this study supports the development of a cost-effective hybrid manufacturing route for producing functional, customized stainless-steel parts that are used in biomedical implants, aerospace, and automotive applications. Most prior research studies have concentrated on as-printed or as-sintered properties, leaving a clear gap in understanding how these parameters affect machinability and post-processed surface quality. The prior studies have also reported the impact of raster angles, layer thickness, and build orientation; only a few have employed systematic statistical analysis to separate significant effects from noise. This knowledge gap is critical because surface finish strongly impacts fatigue performance, corrosion resistance, and overall part functionality. Our study investigates how printing parameters impact the micromilled surface roughness of FDM/FFF 316L stainless steel, thereby providing insights for optimizing hybrid additive- subtractive manufacturing workflows.

Methodology

In the present study, components were fabricated using the Fused Filament Fabrication (FFF) or Fused Deposition Modeling (FDM) process with a MakerBot Method X 3D printer. The workflow began with the development of a computer-aided design (CAD) model, which was exported in the STL format to ensure compatibility with the 3D printer. The material used was a composite filament consisting of 80% 316L stainless steel powder and 20% resin, with a diameter of 1.75 mm. Before printing, the build plate was cleaned of residual material and treated with Magigoo Pro Metal 3D bed adhesive, specifically formulated for BASF Ultrafuse 316L. The printer is equipped with dual extruders: one for the primary metallic filament and the other for support material. A laboratory-scale extruder, designed primarily for metal filaments, was also employed during fabrication. As illustrated in Figure 1, specimens were printed in two build orientations: flat (horizontal) and on-edge (vertical). Printing parameters included layer thicknesses of 0.2 mm and 0.1 mm, an extrusion temperature of 245 °C, a chamber temperature of 85 °C, 100% infill with a linear pattern, and a travel speed of 250 mm/s. Specimens were printed at raster angles of 0°, 30°, and 45°, as shown in Figure 2. After fabrication, the printed parts underwent thermal debinding and sintering to prepare them for machining. The thermal post-processing was carried out by DSH Technologies, LLC. Micromilling operations were then conducted on the sintered specimens. A cutter of 0.063-inch diameter was used in the milling process. The cutting directions were 0°, 90°, and 180° with the horizontal direction of the machined workpiece. The cutting path is explained in Figure 3. At each layer thickness, 6 samples were produced: three printed in the horizontal orientation and three in the vertical orientation. For each orientation, two samples were printed at each raster angle of 0°, 30°, and 45°. Roughness measurements were performed at 0°, 90°, and 180° using a Mitutoyo SurfTest/Portable Surface Roughness tester. The results recorded are shown in Figures 4, 5, 6, and 7.

The micromilling was carried out only on the top (XY) surface of the parts, regardless of whether they were printed in the horizontal or vertical orientation. The initial printing process leaves behind differences in surface waviness, porosity distribution, and

layer bonding that remain even after sintering. These features influence how the cutting tool engages with the material during milling. As a result, parts printed with a larger layer thickness (0.2 mm) still tend to produce rougher surfaces compared to those printed with finer layers (0.1 mm). In other words, the effect of layer height on roughness is indirect. It is not simply a matter of stair-steps being removed, but rather the underlying microstructural variations created during printing and sintering that continue to affect the final machined finish.

The micromilling was carried out using a 0.063-inch (1.6 mm) diameter end mill on the top (XY) surface of the sintered specimens. A constant spindle speed of 2000 rpm, a feed rate of 152.4 mm/min, and a depth of cut of 0.2 mm were used for all samples to maintain uniform conditions. Each sample was machined along three tool paths (0° , 90° , and 180° relative to the XY surface), as shown in Figure 3, with one pass per direction. The process was stopped after completing these paths to ensure the same amount of material was removed from every part. This way, the control in the experiment was the consistent milling procedure itself; any differences observed in surface roughness came only from the printing parameters (layer thickness, raster angle, and orientation), not from variations in the machining process

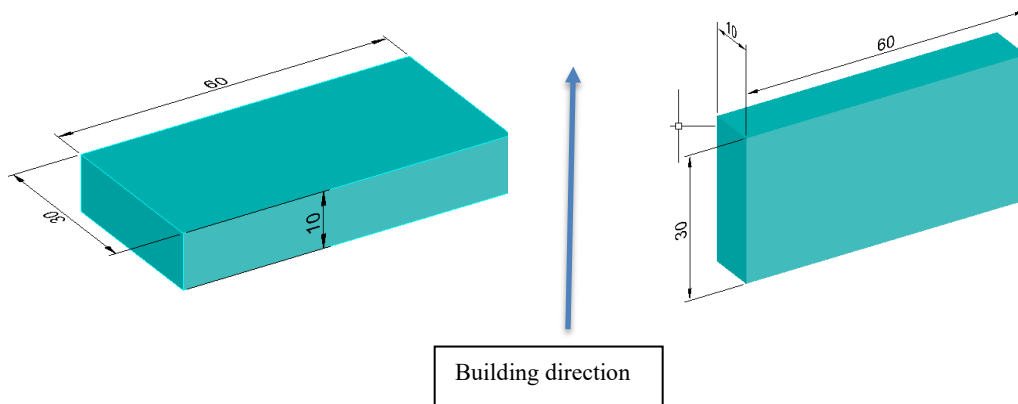


Figure 1: Orientation of the printed samples.

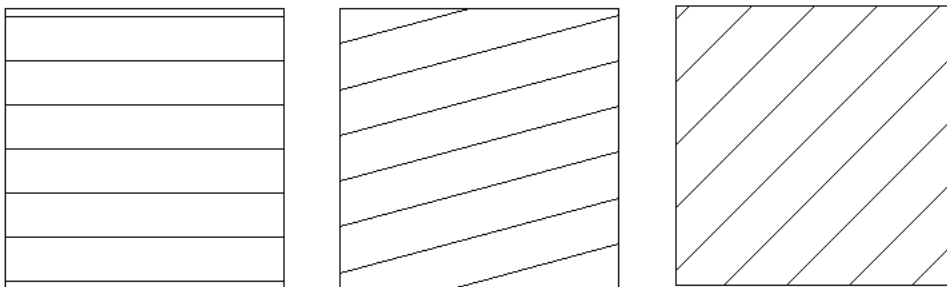


Figure 2: Raster angles (0, 30, and 45).

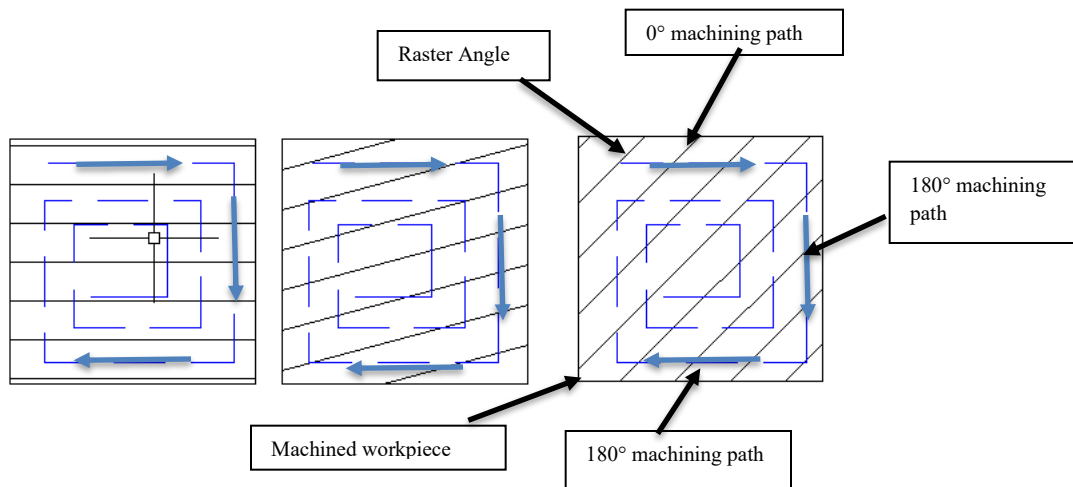


Figure 3: machining paths at 0°, 90°, and 180°

Results and Discussion

All micromilling and profile surface roughness measurements were carried out on the top XY surface of the sintered parts. By focusing only on this surface, we ensured that comparisons between horizontal and vertical builds were valid and avoided confusion between XY and XZ planes. This consistent measurement approach makes it easier to identify how printing parameters influence the final machined surface. This dataset presents the results of surface roughness measurements taken from stainless steel parts produced using Fused Deposition Modeling (FDM) and later machined when the part is at 0° horizontally. For each sample, the raster angle was set to either 0°, 30°, or 45°, while the layer thickness was either 0.1 mm or 0.2 mm. The samples were printed in horizontal and vertical orientations to observe how build direction influences surface quality. All parts were cut while the parts were in the horizontal direction to maintain consistency in the machining setup. The machining operation starts with zero degrees in the horizontal direction, then 90 degrees, and finally with 180 degrees, as shown in Figure 3. Surface roughness was measured in three directions relative to the workpiece direction: directly along it (0°), perpendicular to it (90°), and in the opposite direction (180°) as shown in Figure 3 which shows the workpiece, raster angles and the machining direction. These measurements help highlight how the layer-by-layer nature of 3D printing and the chosen print settings can lead to variations in surface texture, which are important to consider when aiming for precision and quality in final parts. ANOVA is used to study the impact of raster angles, layer thickness, and printing direction on the surface roughness of the machined parts at 0°, 90°, and 180° with the workpiece orientation. The first set of ANOVA analysis is shown in Table 1. Table 1 shows that none of the effects were statistically significant at $\alpha = 0.05$. The interaction between Printing Direction and Layer Thickness had a p-value of 0.075, which is near significance and may indicate a meaningful trend. Raster angle and printing direction alone still do not have significant effects on surface roughness at 0°.

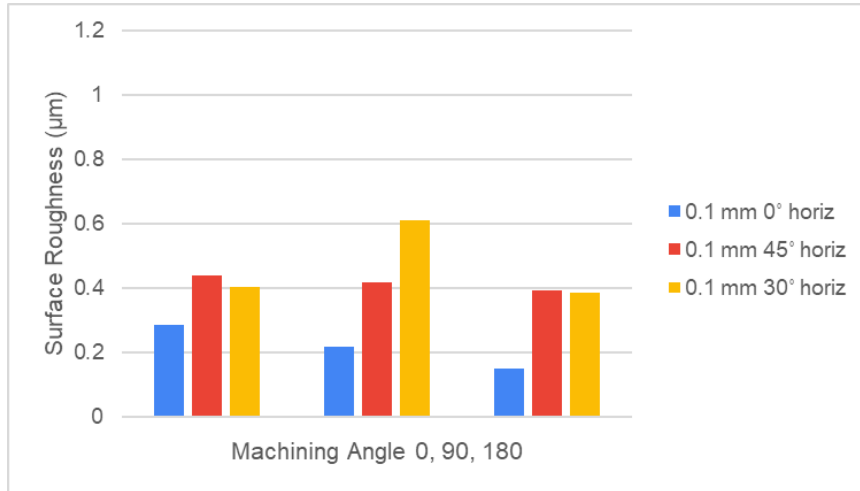


Figure 4: Post-machined surface roughness on the top (XY) surface for 0.1 mm layer thickness, measured at machining directions 0°, 90°, and 180° with raster angles of 0°, 30°, and 45° and horizontal building orientation.

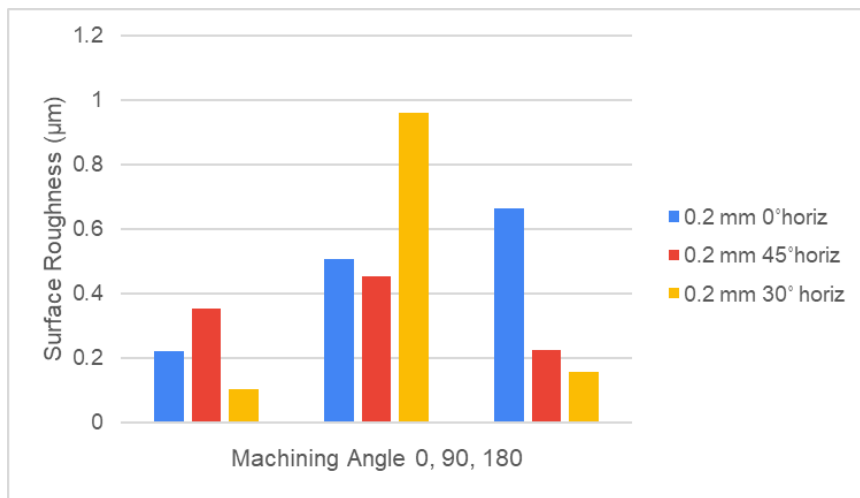


Figure 5: Post-machined surface roughness on the top (XY) surface for 0.2 mm layer thickness, measured at machining directions 0°, 90°, and 180° with raster angles of 0°, 30°, and 45° and horizontal building orientation.

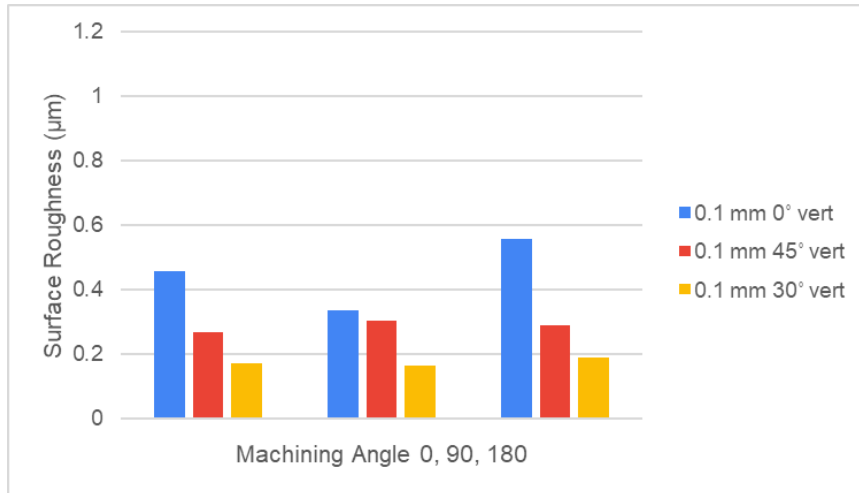


Figure 6: Post-machined surface roughness on the top (XY) surface for 0.1 mm layer thickness, measured at machining directions 0°, 90°, and 180° with raster angles of 0°, 30°, and 45° and vertical building orientation.

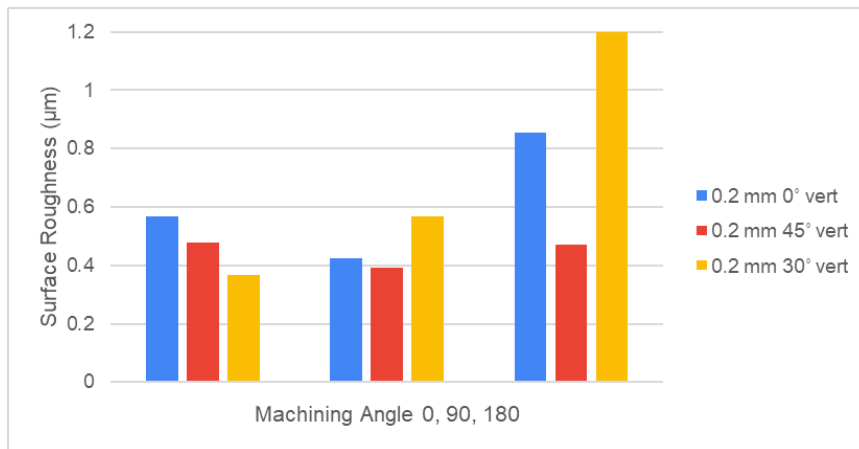


Figure 7: Post-machined surface roughness on the top (XY) surface for 0.2 mm layer thickness, measured at machining directions 0°, 90°, and 180° with raster angles of 0°, 30°, and 45° and vertical building orientation.

Table 1: Analysis of Variance: zero degree cut

Source	DF	Adj SS	Adj MS	F-Value	P-Value
Raster Angle	2	0.039457	0.019729	3.02	0.249
Layer thickness	1	0.000420	0.000420	0.06	0.824
printing direction	1	0.020917	0.020917	3.20	0.216
Raster Angle*Layer thickness	2	0.006663	0.003332	0.51	0.663
Raster Angle*printing direction	2	0.048080	0.024040	3.68	0.214

Layer thickness*printing direction	1	0.077924	0.077924	11.91	0.075
Error	2	0.013080	0.006540		
Total	11	0.206541			

Table 2: Analysis of Variance: 90-degree cut

Source	DF	Adj SS	Adj MS	F-Value	P-Value
Raster Angle	2	0.101029	0.050514	9.25	0.098
Layer thickness	1	0.131880	0.131880	24.15	0.039
printing direction	1	0.078732	0.078732	14.42	0.063
Raster Angle*Layer thickness	2	0.050569	0.025284	4.63	0.178
Raster Angle*printing direction	2	0.103712	0.051856	9.50	0.095
Layer thickness*printing direction	1	0.000833	0.000833	0.15	0.734
Error	2	0.010923	0.005461		
Total	11	0.477678			

Table 3: Analysis of Variance: 180-degree cut

Source	DF	Adj SS	Adj MS	F-Value	P-Value
Raster Angle	2	0.09207	0.04603	0.34	0.745
Layer thickness	1	0.21601	0.21601	1.60	0.333
printing direction	1	0.21121	0.21121	1.57	0.337
Raster Angle*Layer thickness	2	0.10260	0.05130	0.38	0.724
Raster Angle*printing direction	2	0.06446	0.03223	0.24	0.807
Layer thickness*printing direction	1	0.15459	0.15459	1.15	0.396
Error	2	0.26937	0.13468		
Total	11	1.11030			

Since this study was designed as a pilot, the sample size was intentionally limited to get a first look at how FDM printing parameters affect surface roughness after micromilling. As a result, some of the p-values are higher than what is typically expected for statistical significance. These results still reveal interesting trends, especially at the 90° machining direction. This suggests that layer thickness and raster angle could play important roles. The findings aren't conclusive yet, but they point in a clear direction for future more detailed studies. We are in the process of machining the 3D printed parts when the part is tilted at an angle of 30° and 45° to investigate the effect of the printing parameters, such as raster angle, layer thickness, printing orientation, on the surface roughness at 0°, 90°, and 180°. Parts printed with 0.1 mm layer thickness almost always came out smoother after machining compared to those printed with 0.2 mm. This difference was especially noticeable at the 90° machining direction, where the cutting path runs across more interlayer boundaries. Statistical analysis confirmed this observation: ANOVA showed that layer thickness was significant at the 90° direction ($p = 0.039$). At 0° and 180°, the difference between 0.1 mm and 0.2 mm was smaller, but the same trend held. This means that even though the milling process removes the stair-stepped features of the printed surface, the underlying structure created during printing still affects how the cutting tool interacts with the material. Coarser layers leave behind more waviness and porosity after sintering, which makes the final surface rougher, while finer layers produce a more uniform structure and a better finish.

Raster angle also played a role, where when the machining path was (0° or 180°), surface roughness values were fairly similar regardless of whether the raster was set at 0°, 30°, or 45°. However, at the 90° machining direction, where the tool cuts directly across the deposited filaments, 30° and 45° raster angles produced noticeably rougher surfaces than 0°. ANOVA supported this trend, with raster angle approaching statistical significance ($p = 0.098$). This finding highlights the importance of alignment: when the tool path and the deposited raster lines run parallel, the cutter moves more smoothly across the surface. When they are misaligned, the cutter encounters more interlayer boundaries, which increases roughness.

The effect of building orientation also has an important impact on the quality of the machined surface. Horizontal builds tended to produce smoother and more consistent results, while vertical builds showed more scatter in roughness values. Since only the XY surface was measured, this difference cannot be explained by geometry alone; it likely comes from microstructural differences. Vertical builds are more prone to weaker bonding between layers and to anisotropic shrinkage during sintering, both of which introduce variability that shows up during machining. Horizontal builds, on the other hand, provide more stable support and bonding during printing, which makes their machined surfaces more predictable. Although orientation did not show up as statistically significant in the ANOVA, the observed variability is meaningful for practical applications where consistency is important.

By showing that FDM/FFF parameters leave a measurable fingerprint even after machining, this study highlights how optimizing layer thickness, raster alignment, and

build orientation at the printing stage can directly improve the performance and cost-effectiveness of end-use metal components in these demanding applications.

Conclusion

This pilot study offered early insights into how printing parameters such as layer thickness, raster angle, and build orientation can affect the surface roughness of 316L stainless steel parts after micromilling. Not all results reached statistical significance, but some clear patterns began to emerge, especially at the 90° cutting direction, where layer thickness had a noticeable impact and raster angle and printing direction showed promising trends. At 0° and 180°, the results were more varied and did not indicate strong statistical effects, which may be due to the limited sample size and scope of this initial investigation. These findings are valuable as a starting point because they help highlight which parameters are most likely to influence surface quality and where future efforts should focus. Expanding the number of samples and exploring additional cutting angles, when the workpiece is tilted by 30° and 45°, will help build a clearer understanding of how FDM printing parameters interact with the surface roughness of the micromilled surface. One limitation of this study is that only profile roughness parameters were measured, which are direction-dependent. Future work will incorporate areal roughness measurements to provide a more comprehensive and application-oriented assessment of surface quality.

Acknowledgement

This work was funded by Sam Houston State University, Huntsville, Texas.

REFERENCES

- Boschetto, A., Bottini, L., Miani, F., & Veniali, F. (2022). “Roughness investigation of steel 316L parts fabricated by Metal Fused Filament Fabrication.” *Journal of Manufacturing Processes*, *81*, 261–280.
- Caminero, M. A., Romero, A., Chacón, J. M., Núñez, P. J., García-Plaza, E., & Rodríguez, G. P. (2021). Additive manufacturing of 316L stainless-steel structures using fused filament fabrication technology: mechanical and geometric properties. *Rapid Prototyping Journal*, *27*(3), 583–591. doi:10.1108/RPJ-06-2020-0120.
- Cerlincă, D.-A., Tamaşag, I., Beşliu-Băncescu, I., Severin, T.-L., & Dulucianu, C. (2024). Experimental investigation of FDM manufacturing of 316L stainless steel. *The International Journal of Advanced Manufacturing Technology*, *135*, 1449–1463.
- Kedziora, S., Decker, T., Museyibov, E., Morbach, J., Hohmann, S., Huwer, A., & Wahl, M. (2022). Strength properties of 316L and 17-4 PH stainless steel produced with additive manufacturing. *Materials*, *15*(18), 6278. <https://doi.org/10.3390/ma15186278>
- Galati, M., & Minetola, P. (2019). Analysis of density, roughness, and accuracy of the ADAM (metal FFF) process for metal parts. *Materials*, *12*(24), 4122.

- Liu, B., Wang, Y., Lin, Z., & Zhang, T. (2020). Creating metal parts by fused deposition modeling and sintering. *Materials Letters*, *263*, 127252. doi:10.1016/j.matlet.2019.127252
- Martignoni, L., Vegro, A., Candidori, S., Shaikh, M. Q., Atre, S. V., Graziosi, S., & Casati, R. (2024). Prototyping and characterisation of 316L stainless steel parts and lattice structures printed via metal fused filament fabrication. *Rapid Prototyping Journal*, *30*(11), 123–141. doi:10.1108/RPJ-06-2023-0194.
- Obeidat, S., Basith, I., & Dakeev, U. (2024). The impact of printing direction and raster angle on the apparent density and mechanical properties of 316L stainless steel parts printed by FDM/FFF technology. *International Journal of Modern Engineering*, *24*(2), 29–35.
- O'Connor, H., Singh, G., Kumar, A., Paetzold, R., Celikin, M., & O'Cearbhaill, E. D. (2024). Fused filament fabrication using stainless steel 316L–polymer blend: Analysis and optimization for green density and surface roughness. *Polymer Composites*, *45*(12), 10632–10644. doi:10.1002/pc.28496.
- Ren, L., Zhou, X., Song, Z., Zhao, C., Liu, Q., Xue, J., & Li, X. (2017). Process parameter optimization of extrusion-based 3D metal printing utilizing PW–LDPE–SA binder system. *Materials*, *10*(3), 305. <https://doi.org/10.3390/ma10030305>
- Spiller, S., Kolstad, S. O., & Razavi, N. (2023). Fabrication and characterization of 316L stainless steel components printed with material extrusion additive manufacturing. *Procedia Structural Integrity*, *42*, 1239–1248. <https://doi.org/10.1016/j.prostr.2022.12.158>.